ELSEVIER

Biochimica et Biophysica Acta, 1365 (1998) 151–158

BIOCHIMICA ET BIOPHYSICA ACTA
BBA

Structural basis of functions of the mitochondrial cytochrome *bc*1 complex

Chang-An Yu[a,*], Di Xia[b], Hoeon Kim[b], Johann Deisenhofer[b], Li Zhang[a], Anatoly M. Kachurin[a], Linda Yu[a]

[a]*Department of Biochemistry and Molecular Biology, Oklahoma State University, Stillwater, OK 74078-3035, USA*
[b]*Howard Hughes Medical Institute and Department of Biochemistry, University of Texas Southwestern Medical Center, Dallas, TX 75235-9050, USA*

Received 4 February 1998; accepted 23 February 1998

Abstract

The crystal structure of the cytochrome *bc*1 complex (ubiquinol–cytochrome *c* reductase) from bovine heart submitochondria was determined at 2.9 Å resolution. The *bc*1 complex in crystal exists as a closely interacting dimer, suggesting that the dimer is a functional unit. Over half of the mass of the complex, including subunits core 1 and core 2, are on the matrix side of the membrane, while most of the cytochrome *b* subunit is located within the membrane. There are 13 transmembrane helices in each monomer, eight of them belonging to cytochrome *b*. Two large cavities are made of the transmembrane helices D, C, F and H in one monomer and helices D′ and E′ from the other monomer of cytochrome *b*, and the transmembrane helices of *c*1, iron–sulfur protein (ISP), and subunits 10 and 11. These cavities provide entrances for ubiquinone or inhibitor and connect the Q_i pocket of one monomer and the Q_o pocket of the other monomer. Ubiquinol made at the Q_i site of one monomer can proceed to the nearby Q_o site of the other monomer without having to leave the *bc*1 complex. The soluble parts of cytochrome *c*1 and ISP, including their redox prosthetic groups, are located on the cytoplasmic side of the membrane. The distances between the four redox centers in the complex have been determined, and the binding sites for several electron transfer inhibitors have been located. Structural analysis of the protein/inhibitor complexes revealed that the extramembrane domain of the Rieske iron–sulfur protein may undergo substantial movement during the catalytic cycle of the complex. The Rieske protein movement and the larger than expected distance between FeS and cytochrome *c*1 heme suggest that electron transfer reaction between FeS and cytochrome *c*1 may involve movements or conformational changes in the soluble domain of iron–sulfur protein. The inhibitory function of E-β-methoxyacrylate–stilbene and myxothiazol may result from the increase of mobility in ISP, whereas the function of stigmatellin and 5-undecyl-6-hydroxy-4,7-dioxobenzothiazole may result from the immobilization of ISP. © 1998 Elsevier Science B.V.

Keywords: Structure of the cytochrome *bc*1 complex; Electron transfer reaction; Electron transfer inhibitor

1. Introduction

The cytochrome *bc*1 complex (commonly known as ubiquinol–cytochrome *c* reductase or Complex III) is a segment of the mitochondrial respiratory chain that catalyzes antimycin-sensitive electron transfer from ubiquinol to cytochrome *c* [18,10]. The reaction is coupled to the translocation of protons across the mitochondrial inner membrane to generate a proton gradient and membrane potential for ATP synthesis. The purified cytochrome *bc*1 complex contains eleven protein subunits with known amino acid

*Corresponding author: Fax: 405 744 7799.

0005-2728/98/$19.00
PII: S0005-2728(98)00055-3

sequences. The complex consists of 2165 amino acid residues and four prosthetic groups, with a total molecular mass of 248 kDa without counting the bound phospholipids. The essential redox components of the cytochromes *bc*1 complex are: two *b* cytochromes (*b*565 and *b*562), one *c*-type cytochrome (*c*1), one high potential iron–sulfur cluster (FeS) and a ubiquinone.

Based on biochemical and biophysical investigations of the electron transfer and proton translocation mechanisms, investigators in the field now generally favor the proton motive Q-cycle hypothesis [15,19]. The key feature of the Q-cycle hypothesis is the involvement of two separate binding sites for ubiquinone and ubiquinol: Ubiquinol is first oxidized at the Q_o site near the P side of the inner mitochondrial membrane, and ubiquinone is reduced at the Q_i site near the N side of the membrane. According to the Q-cycle model, one electron is transferred from ubiquinol to the Rieske iron–sulfur center, and then to cytochrome *c* via cytochrome *c*1. The newly generated reactive ubisemiquinone then reduces the low-potential cytochrome *b*566 heme (*b*L). Reduced *b*L rapidly transfers an electron to the high-potential cytochrome *b*562 heme (*b*H), which is located on the opposite side of the membrane. A ubiquinone or ubisemiquinone bound at the Q_i site then oxidizes the reduced *b*H. Proton translocation is the result of deprotonation of ubiquinol at the Q_o site and protonation of ubiquinol at the Q_i site.

In addition to the redox-active protein subunits, mitochondrial cytochrome *bc*1 complex also contains non-redox active proteins, the so-called supernumeral subunits [20]. Since these supernumeral subunits are not present in bacterial cytochrome *bc*1 complexes, their role in the complex has long been assumed to be structural rather than catalytic. Recent studies showed that plant mitochondrial *bc*1 complexes from wheat, potato and spinach have mitochondrial processing peptidase (MPP) activity in addition to electron transfer activity [9]. MPP activity was associated with the core subunits [8,4,7,3] of the plant complex. However, a similar peptidase activity is not detected in the bovine *bc*1 complex, even though the sequences of core protein subunits 1 and 2 are highly homologous with the β and α subunits of MPP [4], respectively. The crystal structure of bovine *bc*1 has revealed a putative MPP active site and a zinc binding motif in the core subunits [22], which are associated with an unidentified polypeptide. When crystalline cytochrome *bc*1 complex is treated with non-ionic detergents, such as Triton X-100 or zwitergen, the electron transfer activity is impaired and MPP activity is observed. Properties of the activated MPP were investigated [5].

In this paper we discuss the structural basis of the electron transfer reaction of beef heart mitochondrial cytochrome *bc*1 complex based on the reported 3-D structural information [22] and new crystallographic observations made on this complex [11].

2. Cytochrome *bc*1 complex functions as a dimer

Most reports in the literature favor the dimeric association of the cytochrome *bc*1 complex, even though isolation of monomeric complex has been documented [17,16]. Crystallographic studies of the *bc*1 complex not only show physical dimeric association (Fig. 1) but also suggest that the dimer is functional. The following structural evidences support the functional dimer hypothesis: First, since the distance of 21 Å between two *b*L hemes in the two symmetry related monomers is the same as that between *b*L and *b*H hemes within a monomer, electron transfer between the two *b*L hemes of the dimer should be possible, especially when the membrane is highly energized. Second, the dimeric cytochrome *bc*1 complex forms two symmetry related cavities in the membrane-spanning region. Although each monomer contains both Q_i and Q_o sites, they cannot communicate with each other within a monomer. In the dimeric form of the *bc*1 complex, each cavity connects the Q_o site of one monomer to the Q_i site of the other, making it possible for a quinone molecule reduced at the Q_i site of one monomer to be oxidized at the nearby Q_o site of the other monomer without having to leave the *bc*1 complex. This is consistent with the activity data showing that one mole of ubiquinone per mole of *c*1 is sufficient for a maximal activity of electron transfer in the isolated succinate cytochrome *c* reductase [23]. Third, in the crystal structure, the head domain of the iron–sulfur protein (ISP) of one monomer interacts with cytochrome *b* of the other monomer (Fig. 1).

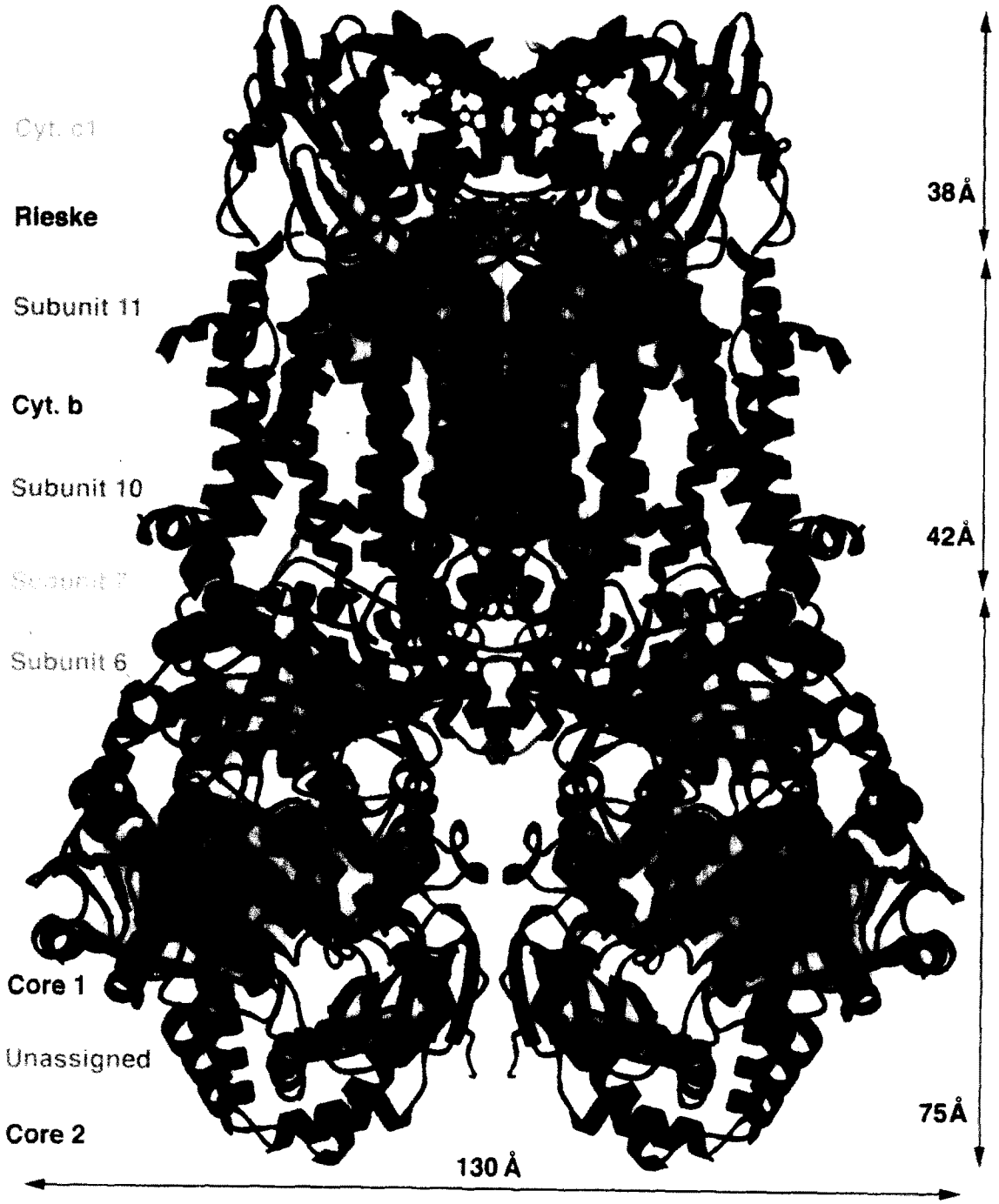

Fig. 1. Partial structure model of the dimeric bovine mitochondrial cytochrome *bc*1 complex. The polypeptides are drawn as ribbons, and heme moieties and iron–sulfur cluster are drawn as the ball-and-stick model. The top of the diagram is in the mitochondrial inter-membrane space, and the bottom is in the mitochondrial matrix space. The molecule can be divided into three regions from the top to bottom: the inter-membrane space region, membrane-spanning region and the matrix region. The dimensions for each region of the molecule and the color code for each subunit are indicated. The unassigned peptide in between subunits core 1 and core 2 is most likely subunit 9. The diagram is produced with the program Setor.

3. Inhibitor binding and movement of iron–sulfur protein

The binding sites for specific electron transfer inhibitors were determined by difference Fourier analysis between inhibitor-bound and native crystals. The relative locations for antimycin A, myxothiazol, 5-undecyl-6-hydroxy-4,7-dioxobenzothiazole (UHDBT), E-β-methoxyacrylate–stilbene (MOAS) and stigmatellin are depicted in Fig. 2. These data show that the binding site of stigmatellin largely overlaps with that of UHDBT and only partly with that of myxothiazol, and the binding site of myxothiazol largely overlaps with that of MOAS, and only slightly overlaps with UHDBT.

The relatively low electron density of the FeS center as compared to those of the *b*H and *b*L in the anomalous scattering difference maps have indicated that the ISP is somewhat mobile in the crystal [22]. Structural analyses of several inhibitor/*bc*1 complex cocrystals suggest that the mobility of ISP is affected by the binding of Q_o site inhibitors. Myxothiazol and MOAS enhance the mobility of ISP, whereas stigmatellin and UHDBT reduce the mobility of ISP in the crystal, as indicated by the enhancement of electron density of FeS (Fig. 3).

4. Ubiquinone binding sites

The key feature of the Q-cycle mechanism is the involvement of two conceptually separated ubiquinone/ubiquinol binding sites: one for ubiquinone reduction and one for ubiquinol oxidation. Structural analysis of the *bc*1–inhibitor complexes reveals two separate inhibitor binding pockets, located at opposite sides of the membrane, for Q_o and Q_i site inhibitors. Binding of the Q_i site inhibitor, antimycin, may cause dislocation of bound Q at the Q_i site, as suggested by a negative electron density in the difference Fourier map between inhibitor-bound and native crystals. Binding of the Q_o site inhibitors, however, does not generate such a negative electron density in the difference maps, indicating that ubiquinone may not be bound in the Q_o pocket in the native crystal. The failure to detect bound ubiquinone at the Q_o pocket may be due to the low binding affinity of the Q_o site for oxidized Q or to the fact that the cytochrome *bc*1 complex used for crystallization contains sub-stoichiometric amounts of Q (~0.6 mole per mole of complex) [24]. How many Q molecules are bound to the Q_o site is a question to be answered in the future. Binding of two Q per Q_o site in bacterial cytochrome *bc*1 complex has been indicated by EPR characteristics of the iron–sulfur cluster [6,2].

The observations that different Q_o site inhibitors bind at slightly different locations in the Q_o pocket and show different effects on ISP encourage us to speculate that there may be two Q binding sites within the Q_o pocket, depending on its redox states, with the fully reduced form being closer to ISP (when FeS is in the oxidized state) and the half reduced form being closer to *b*L (when *b*L is in the oxidized state). In other words, the Q binding site closer to the ISP in the Q_o pocket has higher binding affinity for fully reduced Q and the site closer to *b*L has higher binding affinity for ubisemiquinone. How cytochrome *b* senses such a shift in Q binding positions and subsequently releases ISP requires further structural investigation.

5. Electron transfer rate and distances between the redox centers

The distances of 21 Å between *b*L and *b*H and 27 Å between *b*L and FeS accommodate well the fast electron transfers observed between the two involved redox centers, assuming that ubiquinol is bound between *b*L and FeS. However, the distance of 31 Å between heme *c*1 and FeS, is difficult to explain in view of the large electron transfer rate between these two redox centers. One possible explanation is that movement of ISP may facilitate the observed fast electron transfer in this region in the following way: The iron–sulfur cluster (FeS) is reduced at a position 27 Å from *b*L and 31 Å from cytochrome *c*1. Once reduced, it moves closer to cytochrome *c*1, to donate its electron. The iron–sulfur cluster reduced by the first electron of ubiquinol either cannot donate an electron to cytochrome *c*1 before the second electron of ubiquinol is transferred to cytochrome *b*L, or the reoxidized ISP (after transfer of an electron to *c*1) cannot get back to cytochrome *b* to get re-reduced before the second electron being transferred to *b*L. It

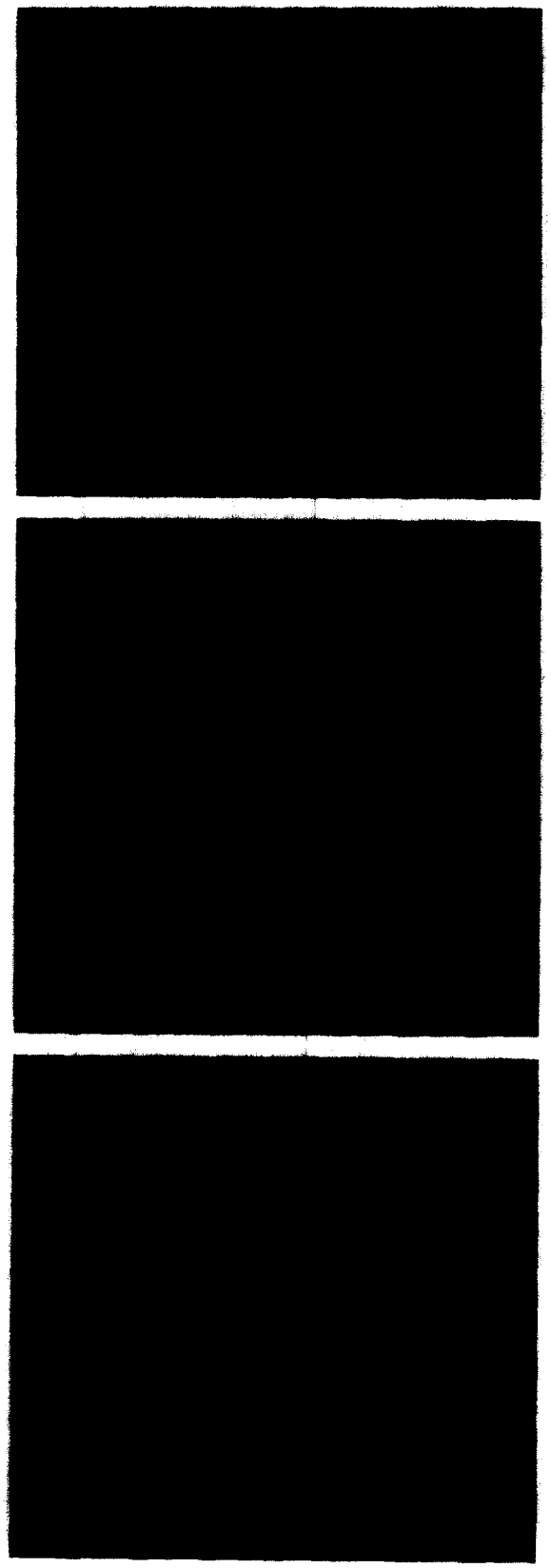

Fig. 2. Iron positions from anomalous diffraction experiment from the *bc*1 complex crystal and locations of difference electron density for inhibitors in cytochrome *b*. The anomalous diffraction peaks for the irons are in red and the peak assignments are indicated. Antimycin A in green, the Q_i site inhibitor, is bound near *b*H heme iron. UHDBT in blue and MOAS in coral are both bound in the Q_o pocket between FeS and *b*L but in two separate binding sites. (a) Front view, (b) rotation of 90° along the two-fold molecular axis and (c) top view from the inter-membrane space.

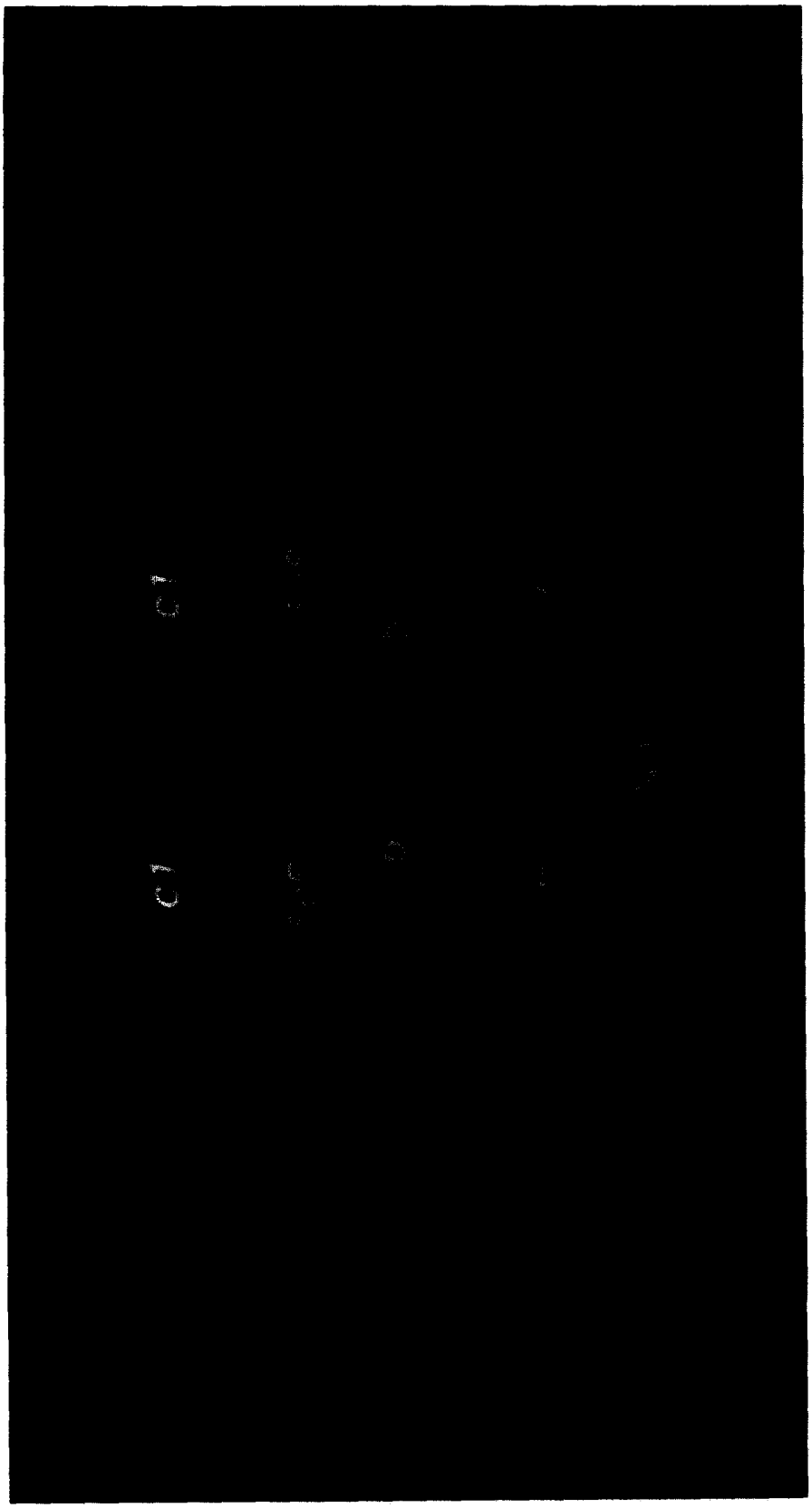

Fig. 3. Effects of inhibitor binding on the anomalous, electron density peak of the FeS cluster. Iron peaks from anomalous diffraction experiments with and without bound inhibitors are shown, with the MOAS-bound crystal on the left, stigmatellin on the right and the native in the middle. Peak assignments are indicated for native only. The iron peak height of bH heme for each crystal is normalized to that for the native. Different inhibitors produce significant changes in the peak height for FeS. Stigmatellin makes the FeS peak much higher at the native position than that for the native, indicating a stabilization effect on the Rieske subunit upon binding. MOA–stilbene, on the other hand, completely destroys the anomalous peak for FeS at the native position, suggesting a destabilization effect upon binding. It is also noticed that there appeared to be a very small peak near c1 iron upon the binding of MOAS; this peak may suggest a preferred binding site near cytochrome c1.

is tempting to speculate that the change of the Q binding site and reduction of *b*L causes a conformational change in cytochrome *b* that allows ISP to move close enough to heme *c*1 to have fast electron transfer [13,21]. This model also would explain why ubisemiquinone, a more powerful reductant, reduces *b*L, but not FeS, during quinol oxidation. This speculation is in line with the observed effect of Q_o site inhibitors binding on the mobility of ISP [11].

6. Electron transfer events at the Q_o site

One of the most important features of the Q cycle hypothesis is the bifurcation of electron transfer at the Q_o site, the mechanism of which is still under intensive investigation. The information from crystal structure and from crystallographic inhibitor studies suggests two transient quinone binding sites in the inhibitor binding pocket at the Q_o site: one Q binding site is likely to be where UHDBT binds, closer to ISP and designated as P1; the other Q binding site is where MOAS binds, closer to *b*L heme and designated as P2. Analogous to inhibitor binding, binding of Q to P1 will cause ISP to be less mobile, and binding of Q to P2 will release ISP. Therefore, the electron transfer events at the Q_o site can be described (Fig. 4) as follows: A ubiquinol molecule comes in, first binds to the P1 site, ISP is immobilized, one proton is released followed by transfer of one electron to ISP. After the second proton is released, the ubisemiquinone radical moves from the P2 site, which causes the ISP to be released, and prevents the remaining electron from going to ISP. The second electron of quinol (ubisemiquinone) then reduces the *b*L heme. This completes the cycle in a manner similar to that in the proposed catalytic switch model [1]. This model requires that the P1 site has a higher affinity for ubiquinol when FeS is in the oxidized state, and that the P2 site has a higher affinity for ubisemiquinone when *b*L is in the oxidized state. The bifurcation of electron transfer at the Q_o site is therefore realized by the large movement of the ISP. The movement is induced by the binding of different redox states of Q at two different subsites in the Q_o binding pocket. The lack of detectable ubisemiquinone radical at the Q_o site, however, is inconsistent with this proposed electron transfer.

An alternative hypothesis for the electron transfer

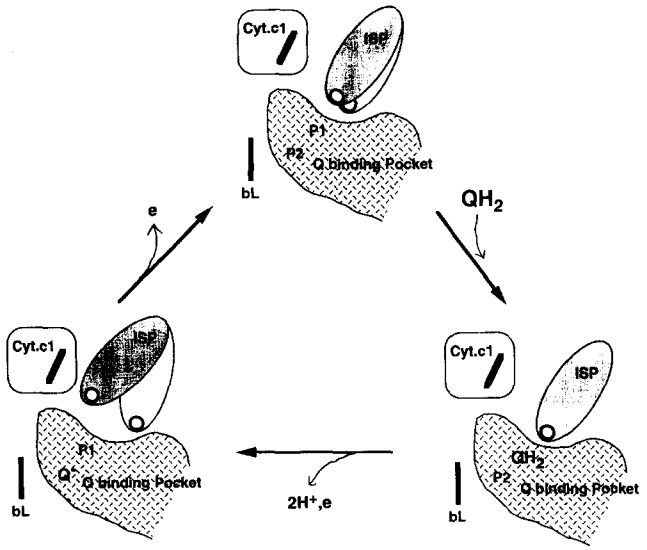

Fig. 4. Schematic diagram of the electron transfer events at the Q_o site. When *bc*1 is in the oxidized form, the ISP prefers the position near cytochrome *b* and is slightly tumbling at that position. Once a ubiquinol molecule gets into the Q_o pocket, it first occupies the P1 site, fixing ISP in place, presumably by a conformational change in cytochrome *b*. The stabilization of ISP facilitates the transfer of the first electron from ubiquinol to ISP and releases two protons. The resulting ubisemiquinone is then switched to the second binding site, P2. This switch in position and the subsequent electron transfer from *b*L to *b*H heme may cause a conformational change in cytochrome *b* and, thus, result in the release of the reduced ISP to a second position near cytochrome *c*1 to deliver its electron.

event at the Q_o site is that the electron donor of FeS is the ubiquinol heme bL^{3+} complex and not the ubiquinol alone. Once the first electron of ubiquinol in the complex transfers to FeS, the second electron immediately transfers to heme *b*L and then to heme *b*H and thus no semiubiquinone is generated. The electron transfer from heme *b*L to heme *b*H results in a conformational change of cytochrome *b* protein which makes (or allows) the reduced ISP to move to a position closer to heme *c*1 to allow electron transfer to take place. Since the oxidation of the reduced FeS depends on the transfer of the second electron of ubiquinol from heme *b*L to heme *b*H, bifurcation is obligatory for the oxidation of ubiquinol in the *bc*1 complex.

7. Proton translocation: pumping/gating

Although the Q cycle hypothesis explains well the $2H^+$–electron stoichiometry of proton transfer and the structural information obtained so far generally

supports this hypothesis, the proton transfer path in the *bc*1 molecule during ubiquinol oxidation is still not clear. No obvious proton channel was found in the cytochrome *bc*1 complex at the current level of structure resolution. This, of course, does not exclude the participation of bound water in proton movement. Since the simplest bacterial *bc*1 complex has no supernumeral subunits and has full proton translocation ability, proton translocation must be achieved through transmembrane helices of cytochrome *b*, *c*1 and ISP. Van der Waals surface of the matrix side of these transmembrane helices, particularly in cytochrome *b*, shows several openings for proton uptake from the matrix. Since the Van der Waals surface of the cytoplasmic side is totally sealed, proton exit must be accompanied by some sort of conformational change or gating device. The available biochemical data indicate that the iron–sulfur cluster of ISP may play an essential role in proton exit. It was reported that the FeS of ISP in the *bc*1 complex can be destroyed by the destruction of one of the histidine ligands during illumination of the hematoporphyrin-treated complex ([14]). The resulting complex leaks protons when reconstituted into phospholipid vesicles. A strong redox state-dependent pK_a of the histidyl ligands of FeS cluster also suggests that they may be involved in proton release [12]. Cytochrome *bc*1 complex depleted in iron–sulfur protein, prepared by biochemical methods or by genetic manipulation, forms proton leaking vesicles when embedded in phospholipid vesicles. These results also support the above speculation.

Acknowledgements

The work described in this review was supported in part by a grant from the National Institutes of Health (GM 30721 to CAY) and from the Welch Foundation (to JD). JD is an investigator in the Howard Hughes Medical Institute. This publication is approved by the director of the Agricultural Experiment Station, Oklahoma State University.

References

[1] U. Brandt, G. Von Jagow, Eur. J. Biochem. 195 (1991) 163–170.
[2] U. Brandt, S. Uribe, H. Schagger, B.L. Trunpower, J. Biol. Chem. 269 (1994) 12947–12953.
[3] H.P. Braun, M. Emmermann, V. Kraft, U.K. Schmitz, EMBO J. 11 (1992) 3219–3227.
[4] H.-P. Braun, U.K. Schmitz, Trends Biochem. Sci. (1995) 171–175.
[5] K.-P. Deng, D. Xia, A.M. Kachurin, H. Kim, J. Deisenhofer, L. Yu, C.A. Yu, Biophys. J. 72 (1997) 319a.
[6] H. Ding, C.C. Moser, D.E. Robertson, M.K. Tokito, F. Daldal, L.P. Dutton, Biochemistry 34 (1995) 15979–15996.
[7] A.C. Eriksson, S. Sjoling, E. Glaser, Biochim. Biophys. Acta 1186 (1994) 221–231.
[8] A.C. Eriksson, S. Sjoling, E. Glaser, J. Bioenerg. Biomembr. 28 (1996) 283–290.
[9] E.G. Glaser, A.R. Crofts, Biochim. Biophys. Acta 766 (1984) 322–333.
[10] Y. Hatefi, A.G. Haavik, D.E. Griffiths, J. Biol. Chem. 237 (1962) 1681–1685.
[11] H. Kim, D. Xia, J. Deisenhofer, C.A. Yu, A. Kachurin, L. Zhang, L. Yu, FASEB J. 11 (1997) 1084a.
[12] T.A. Link, S. Iwata, Biochim. Biophys. Acta 1275 (1996) 54–60.
[13] S.W. Meinhardt, A.R. Crofts, FEBS Lett. 149 (1982) 223–227.
[14] T. Miki, L. Yu, C.A. Yu, Biochemistry 30 (1990) 230–238.
[15] P. Mitchell, J. Theor. Biol. 62 (1976) 327–367.
[16] A. Musatov, N.C. Robinson, Biochemistry 33 (1994) 13005–13012.
[17] M.J. Nalecz, A. Azzi, Arch. Biochem. Biophys. 236 (1985) 619–628.
[18] J.S. Rieske, Methods Enzymol. 10 (1967) 239–245.
[19] B.L. Trumpower, J. Biol. Chem. 265 (1990) 11409–11412.
[20] B.L. Trumpower, Microbiol. Rev. (1990b) 101–129.
[21] A.L. Tsai, J.S. Olson, G. Palmer, J. Biol. Chem. 258 (1983) 2122–2125.
[22] D. Xia, C.A. Yu, H. Kim, J.-Z. Xia, A.M. Kachurin, L. Zhang, L. Yu, J. Deisenhofer, Science 277 (1997) 60–66.
[23] C.A. Yu, L. Yu, Biochim. Biophys. Acta 639 (1981) 99–128.
[24] W.H. Yue, L. Yu, C.A. Yu, Biochemistry 30 (1991) 230–233.